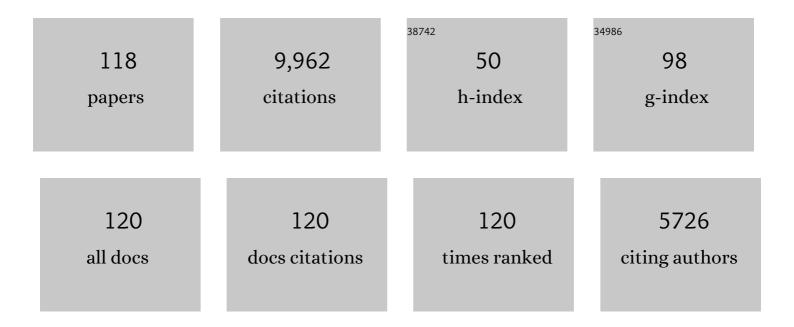
Stephen F Foley

List of Publications by Year in descending order

Source: https://exaly.com/author-pdf/1201763/publications.pdf Version: 2024-02-01



#	Article	IF	CITATIONS
1	Growth of early continental crust controlled by melting of amphibolite in subduction zones. Nature, 2002, 417, 837-840.	27.8	885
2	Vein-plus-wall-rock melting mechanisms in the lithosphere and the origin of potassic alkaline magmas. Lithos, 1992, 28, 435-453.	1.4	600
3	Rutile/melt partition coefficients for trace elements and an assessment of the influence of rutile on the trace element characteristics of subduction zone magmas. Geochimica Et Cosmochimica Acta, 2000, 64, 933-938.	3.9	514
4	Structural characterization of Nigerian coals by X-ray diffraction, Raman and FTIR spectroscopy. Energy, 2010, 35, 5347-5353.	8.8	418
5	Rejuvenation and erosion of the cratonic lithosphere. Nature Geoscience, 2008, 1, 503-510.	12.9	305
6	Genesis of Ultramafic Lamprophyres and Carbonatites at Aillik Bay, Labrador: a Consequence of Incipient Lithospheric Thinning beneath the North Atlantic Craton. Journal of Petrology, 2006, 47, 1261-1315.	2.8	289
7	Enhanced Role of Transition Metal Ion Catalysis During In-Cloud Oxidation of SO ₂ . Science, 2013, 340, 727-730.	12.6	286
8	Petrological characterization of the source components of potassic magmas: geochemical and experimental constraints. Lithos, 1992, 28, 187-204.	1.4	254
9	Minor and trace elements in olivines as probes into early igneous and mantle melting processes. Earth and Planetary Science Letters, 2013, 363, 181-191.	4.4	254
10	A Reappraisal of Redox Melting in the Earth's Mantle as a Function of Tectonic Setting and Time. Journal of Petrology, 2011, 52, 1363-1391.	2.8	242
11	Craton reactivation on the Labrador Sea margins: 40Ar/39Ar age and Sr–Nd–Hf–Pb isotope constraints from alkaline and carbonatite intrusives. Earth and Planetary Science Letters, 2007, 256, 433-454.	4.4	234
12	Trace element partition coefficients for clinopyroxene and phlogopite in an alkaline lamprophyre from Newfoundland by LAM-ICP-MS. Geochimica Et Cosmochimica Acta, 1996, 60, 629-638.	3.9	231
13	Between carbonatite and lamproite—Diamondiferous Torngat ultramafic lamprophyres formed by carbonate-fluxed melting of cratonic MARID-type metasomes. Geochimica Et Cosmochimica Acta, 2008, 72, 3258-3286.	3.9	221
14	Parallels in the origin of the geochemical signatures of island arc volcanics and continental potassic igneous rocks: The role of residual titanates. Chemical Geology, 1990, 85, 1-18.	3.3	204
15	Evolution of the Archaean crust by delamination and shallow subduction. Nature, 2003, 421, 249-252.	27.8	200
16	The Palaeoanthropocene – The beginnings of anthropogenic environmental change. Anthropocene, 2013, 3, 83-88.	3.3	178
17	Integrating Ultramafic Lamprophyres into the IUCS Classification of Igneous Rocks: Rationale and Implications. Journal of Petrology, 2005, 46, 1893-1900.	2.8	173
18	Experimentally determined partitioning of high field strength- and selected transition elements between spinel and basaltic melt. Chemical Geology, 1994, 117, 193-218.	3.3	172

#	Article	IF	CITATIONS
19	An essential role for continental rifts and lithosphere in the deep carbon cycle. Nature Geoscience, 2017, 10, 897-902.	12.9	150
20	Tertiary Ultrapotassic Volcanism in Serbia: Constraints on Petrogenesis and Mantle Source Characteristics. Journal of Petrology, 2005, 46, 1443-1487.	2.8	145
21	Potassic and ultrapotassic magmas and their origin. Lithos, 1992, 28, 181-185.	1.4	141
22	Partial melting in Archean subduction zones: constraints from experimentally determined trace element partition coefficients between eclogitic minerals and tonalitic melts under upper mantle conditions. Precambrian Research, 2002, 113, 323-340.	2.7	133
23	Recycling plus: A new recipe for the formation of Alpine–Himalayan orogenic mantle lithosphere. Earth and Planetary Science Letters, 2013, 362, 187-197.	4.4	133
24	High-pressure stability of the fluor- and hydroxy-endmembers of pargasite and K-richterite. Geochimica Et Cosmochimica Acta, 1991, 55, 2689-2694.	3.9	130
25	Evidence for Archean ocean crust with low high field strength element signature from diamondiferous eclogite xenoliths. Lithos, 1999, 48, 317-336.	1.4	108
26	The olivine macrocryst problem: New insights from minor and trace element compositions of olivine from Lac de Gras kimberlites, Canada. Lithos, 2015, 220-223, 238-252.	1.4	104
27	δ ³⁰ Si and δ ²⁹ Si Determinations on USGS BHVOâ€1 and BHVOâ€2 Reference Materials with a New Configuration on a Nu Plasma Multi ollector ICPâ€MS. Geostandards and Geoanalytical Research, 2008, 32, 193-202.	1.9	101
28	An experimental study of olivine lamproite: First results from the diamond stability field. Geochimica Et Cosmochimica Acta, 1993, 57, 483-489.	3.9	95
29	Torngat ultramafic lamprophyres and their relation to the North Atlantic Alkaline Province. Lithos, 2004, 76, 491-518.	1.4	93
30	Experimental constraints on phlogopite chemistry in lamproites: 1. The effect of water activity and oxygen fugacity. European Journal of Mineralogy, 1989, 1, 411-426.	1.3	89
31	Low Ni olivine in silica-undersaturated ultrapotassic igneous rocks as evidence for carbonate metasomatism in the mantle. Earth and Planetary Science Letters, 2016, 444, 64-74.	4.4	86
32	Metasomatized lithospheric mantle for Mesozoic giant gold deposits in the North China craton. Geology, 2020, 48, 169-173.	4.4	85
33	The role of fluorine and oxygen fugacity in the genesis of the ultrapotassic rocks. Contributions To Mineralogy and Petrology, 1986, 94, 183-192.	3.1	83
34	The effect of fluorine on phase relationships in the system KAlSiO4-Mg2SiO4-SiO2 at 28 kbar and the solution mechanism of fluorine in silicate melts. Contributions To Mineralogy and Petrology, 1986, 93, 46-55.	3.1	83
35	Trace element compositions of minerals in garnet and spinel peridotite xenoliths from the Vitim volcanic field, Transbaikalia, eastern Siberia. Lithos, 1999, 48, 263-285.	1.4	80
36	Contrasting types of metasomatism in dunite, wehrlite and websterite xenoliths from Kimberley, South Africa. Geochimica Et Cosmochimica Acta, 2008, 72, 5722-5756.	3.9	78

#	Article	IF	CITATIONS
37	Kimberlite genesis from a common carbonate-rich primary melt modified by lithospheric mantle assimilation. Science Advances, 2020, 6, eaaz0424.	10.3	72
38	Low-pressure fractionation of the Nyiragongo volcanic rocks, Virunga Province, D.R. Congo. Journal of Volcanology and Geothermal Research, 2004, 136, 269-295.	2.1	71
39	Liquid immiscibility and melt segregation in alkaline lamprophyres from Labrador. Lithos, 1984, 17, 127-137.	1.4	69
40	Continuous cratonic crust between the Congo and Tanzania blocks in western Uganda. International Journal of Earth Sciences, 2010, 99, 1559-1573.	1.8	68
41	Trace element variations in olivine phenocrysts from Ugandan potassic rocks as clues to the chemical characteristics of parental magmas. Contributions To Mineralogy and Petrology, 2011, 162, 1-20.	3.1	67
42	Paleo-Asian oceanic slab under the North China craton revealed by carbonatites derived from subducted limestones. Geology, 2016, 44, 1039-1042.	4.4	67
43	Partitioning of rare earth elements, Y, Th, U, and Pb between pargasite, kaersutite, and basanite to trachyte melts: Implications for percolated and veined mantle. Geochemistry, Geophysics, Geosystems, 2000, 1, n/a-n/a.	2.5	63
44	Trace element partitioning in lamproitic magmas—the Gaussberg olivine leucitite. Lithos, 2004, 75, 19-38.	1.4	63
45	Magmatic modification and metasomatism of the subcontinental mantle beneath the Vitim volcanic field (East Siberia): evidence from trace element data on pyroxenite and peridotite xenoliths from Miocene picrobasalt. Lithos, 2000, 54, 83-114.	1.4	62
46	Laser-ablation ICP-MS analysis of siliceous rock glasses fused on an iridium strip heater using MgO dilution. Mikrochimica Acta, 2008, 160, 153-163.	5.0	62
47	Petrological characterization of the mantle source of Mediterranean lamproites: Indications from major and trace elements of phlogopite. Chemical Geology, 2013, 353, 267-279.	3.3	62
48	Calcium isotope fractionation during magmatic processes in the upper mantle. Geochimica Et Cosmochimica Acta, 2019, 249, 121-137.	3.9	58
49	First direct evidence of sedimentary carbonate recycling in subduction-related xenoliths. Scientific Reports, 2015, 5, 11547.	3.3	57
50	Melting and dynamic metasomatism of mixed harzburgite + glimmerite mantle source: Implications for the genesis of orogenic potassic magmas. Chemical Geology, 2017, 455, 182-191.	3.3	52
51	Trace element partitioning in the granulite facies. Contributions To Mineralogy and Petrology, 2010, 159, 493-519.	3.1	51
52	Non-explosive, dome-forming eruptions at Mt. Taranaki, New Zealand. Geomorphology, 2012, 136, 15-30.	2.6	51
53	Potassium-rich magmatism from a phlogopite-free source. Geology, 2017, 45, 467-470.	4.4	50
54	Displaced cratonic mantle concentrates deep carbon during continental rifting. Nature, 2020, 582, 67-72.	27.8	50

#	Article	IF	CITATIONS
55	Phase relations and fractionation sequences in potassic magma series modelled in the system CaMgSi 2 O 6 -KAlSiO 4 -Mg 2 SiO 4 -SiO 2 -F 2 O â~1 at 1 bar to 18 kbar. Contributions To Mineralogy and Petrology, 2000, 138, 186-197.	3.1	48
56	Sulfur isotope ratio measurements of individual sulfate particles by NanoSIMS. International Journal of Mass Spectrometry, 2008, 272, 63-77.	1.5	46
57	An experimental study of the role of partial melts of sediments versus mantle melts in the sources of potassic magmatism. Journal of Asian Earth Sciences, 2019, 177, 76-88.	2.3	46
58	Early continental crust generated by reworking of basalts variably silicified by seawater. Nature Geoscience, 2019, 12, 769-773.	12.9	45
59	Thermal-chemical conditions of the North China Mesozoic lithospheric mantle and implication for the lithospheric thinning of cratons. Earth and Planetary Science Letters, 2019, 516, 1-11.	4.4	42
60	Fe-rich Dunite Xenoliths from South African Kimberlites: Cumulates from Karoo Flood Basalts. Journal of Petrology, 2007, 48, 1387-1409.	2.8	41
61	Trace elements in olivine of ultramafic lamprophyres controlled by phlogopite-rich mineral assemblages in the mantle source. Lithos, 2017, 292-293, 81-95.	1.4	41
62	Carbonated sediment recycling and its contribution to lithospheric refertilization under the northern North China Craton. Chemical Geology, 2017, 466, 641-653.	3.3	41
63	Experimental constraints on phlogopite chemistry in lamproites: 2. Effect of pressure-temperature variations. European Journal of Mineralogy, 1990, 2, 327-342.	1.3	41
64	Calcium isotope evidence for subduction-enriched lithospheric mantle under the northern North China Craton. Geochimica Et Cosmochimica Acta, 2018, 238, 55-67.	3.9	39
65	Calcium isotopic compositions of oceanic crust at various spreading rates. Geochimica Et Cosmochimica Acta, 2020, 278, 272-288.	3.9	37
66	11. Trace-Element Partitioning Between Amphibole and Silicate Melt. , 2007, , 417-452.		32
67	Metamorphism and melting of picritic crust in the early Earth. Lithos, 2014, 189, 173-184.	1.4	30
68	Generation of continental intraplate alkali basalts and implications for deep carbon cycle. Earth-Science Reviews, 2020, 201, 103073.	9.1	30
69	Constraints on the sources of post-collisional K-rich magmatism: The roles of continental clastic sediments and terrigenous blueschists. Chemical Geology, 2017, 455, 192-207.	3.3	29
70	Subduction-related petrogenesis of Late Archean calc-alkaline lamprophyres in the Yilgarn Craton (Western Australia). Precambrian Research, 2020, 338, 105550.	2.7	29
71	High-pressure synthesis of priderite and members of the lindsleyite-mathiasite and hawthorneite-yimengite series. Contributions To Mineralogy and Petrology, 1994, 117, 164-174.	3.1	28
72	Insights into the petrogenesis of the West Kimberley lamproites from trace elements in olivine. Mineralogy and Petrology, 2018, 112, 519-537.	1.1	28

#	Article	IF	CITATIONS
73	Kimberlites from Source to Surface: Insights from Experiments. Elements, 2019, 15, 393-398.	0.5	28
74	Molecular composition and chemotaxonomic aspects of Eocene amber from the Ameki Formation, Nigeria. Organic Geochemistry, 2012, 51, 55-62.	1.8	27
75	Trace-element partitioning between synthetic potassic-richterites and silicate melts, and contrasts with the partitioning behaviour of pargasites and kaersutites. European Journal of Mineralogy, 2003, 15, 329-340.	1.3	26
76	Experimental investigation of the composition of incipient melts in upper mantle peridotites in the presence of CO2 and H2O. Lithos, 2021, 396-397, 106224.	1.4	24
77	Two-Stage Origin of K-Enrichment in Ultrapotassic Magmatism Simulated by Melting of Experimentally Metasomatized Mantle. Minerals (Basel, Switzerland), 2020, 10, 41.	2.0	23
78	Gold endowment of the metasomatized lithospheric mantle for giant gold deposits: Insights from lamprophyre dykes. Geochimica Et Cosmochimica Acta, 2022, 316, 21-40.	3.9	23
79	Compositional and pressure controls on calcium and magnesium isotope fractionation in magmatic systems. Geochimica Et Cosmochimica Acta, 2020, 290, 257-270.	3.9	22
80	The effect of crystal orientation on the wetting behaviour of silicate melts on the surfaces of spinel peridotite minerals. Contributions To Mineralogy and Petrology, 2002, 143, 254-262.	3.1	21
81	Terpenoid composition and chemotaxonomic aspects of Miocene amber from the Koroglu Mountains, Turkey. Journal of Analytical and Applied Pyrolysis, 2014, 105, 100-107.	5.5	21
82	Massive carbon storage in convergent margins initiated by subduction of limestone. Nature Communications, 2021, 12, 4463.	12.8	21
83	Xenoliths from the sub-volcanic lithosphere of Mt Taranaki, New Zealand. Journal of Volcanology and Geothermal Research, 2010, 190, 192-202.	2.1	20
84	Anatectic amphibole and restitic garnet in Variscan migmatite from NE Sardinia, Italy: insights into partial melting from mineral trace elements. European Journal of Mineralogy, 2014, 26, 381-395.	1.3	20
85	Melting of hydrous pyroxenites with alkali amphiboles in the continental mantle: 1. Melting relations and major element compositions of melts. Geoscience Frontiers, 2022, 13, 101380.	8.4	20
86	Bushveld superplume drove Proterozoic magmatism and metallogenesis in Australia. Scientific Reports, 2020, 10, 19729.	3.3	18
87	The Geochemical Complexity of Kimberlite Rocks and their Olivine Populations: a Comment on Cordier <i>et al.</i> (<i>Journal of Petrology</i> , 56, 1775–1796, 2015). Journal of Petrology, 2016, 57, 921-926.	2.8	16
88	Primary Melt Compositions in the Earth's Mantle. , 2018, , 3-42.		16
89	Evidence for a Carbonatite-Influenced Source Assemblage for Intraplate Basalts from the Buckland Volcanic Province, Queensland, Australia. Minerals (Basel, Switzerland), 2019, 9, 546.	2.0	16
90	Melting of sediments in the deep mantle produces saline fluid inclusions in diamonds. Science Advances, 2019, 5, eaau2620.	10.3	16

#	Article	IF	CITATIONS
91	Early cretaceous lamprophyre dyke swarms in Jiaodong Peninsula, eastern North China Craton, and implications for mantle metasomatism related to subduction. Lithos, 2020, 368-369, 105593.	1.4	16
92	Lithospheric transformation of the northern North China Craton by changing subduction style of the Paleo-Asian oceanic plate: Constraints from peridotite and pyroxenite xenoliths in the Yangyuan basalts. Lithos, 2019, 328-329, 58-68.	1.4	15
93	Platinum group element mobilization in the mantle enhanced by recycled sedimentary carbonate. Earth and Planetary Science Letters, 2020, 541, 116262.	4.4	15
94	Mineral and trace element composition of the Lokpanta oil shales in the Lower Benue Trough, Nigeria. Fuel, 2011, 90, 2843-2849.	6.4	14
95	Hybridization Melting Between Continentâ€Derived Sediment and Depleted Peridotite in Subduction Zones. Journal of Geophysical Research: Solid Earth, 2018, 123, 3414-3429.	3.4	14
96	Petrogenesis of Proterozoic alkaline ultramafic rocks in the Yilgarn Craton, Western Australia. Gondwana Research, 2021, 93, 197-217.	6.0	13
97	Origin of low-MgO primitive intraplate alkaline basalts from partial melting of carbonate-bearing eclogite sources. Geochimica Et Cosmochimica Acta, 2022, 324, 240-261.	3.9	13
98	Sediment-Peridotite Reaction Controls Fore-Arc Metasomatism and Arc Magma Geochemical Signatures. Geosciences (Switzerland), 2021, 11, 372.	2.2	12
99	Thermochemical structure and evolution of cratonic lithosphere in central and southern Africa. Nature Geoscience, 2022, 15, 405-410.	12.9	12
100	Characterisation of chromites, chromite hosted inclusions of silicates and metal alloys in chromitites from the Indo-Myanmar ophiolite belt of Northeastern India. Ore Geology Reviews, 2017, 90, 260-273.	2.7	11
101	Geochemical characteristics of lawsonite blueschists in tectonic mélange from the Tavşanlı Zone, Turkey: Potential constraints on the origin of Mediterranean potassium-rich magmatism. American Mineralogist, 2019, 104, 724-743.	1.9	11
102	A review and assessment of experiments on Kimberlites, Lamproites and Lamprophyres as a guide to their Origin. Journal of Earth System Science, 1990, 99, 57-80.	1.3	10
103	Experimental interaction of granitic melt and peridotite at 1.5â€ [−] GPa: Implications for the origin of post-collisional K-rich magmatism in continental subduction zones. Lithos, 2019, 350-351, 105241.	1.4	10
104	Rutile records for the cooling history of the Trans-North China orogen from assembly to break-up of the Columbia supercontinent. Precambrian Research, 2020, 346, 105763.	2.7	10
105	Mantle rocks in East Antarctica. Geological Society Memoir, 2023, 56, 17-32.	1.7	8
106	Origin of potassic postcollisional volcanic rocks in young, shallow, blueschist-rich lithosphere. Science Advances, 2021, 7, .	10.3	7
107	Trace element compositions of minerals in garnet and spinel periodotite xenoliths from the Vitim volcanic field, Transbaikalia, eastern Siberia. Developments in Geotectonics, 1999, 24, 263-285.	0.3	6
108	Petrology of spinel lherzolite xenoliths from Youkou volcano, Adamawa Massif, Cameroon Volcanic Line: mineralogical and geochemical fingerprints of sub-rift mantle processes. Contributions To Mineralogy and Petrology, 2018, 173, 1.	3.1	6

0

#	Article	IF	CITATIONS
109	Variation in mantle lithology and composition beneath the Ngao Bilta volcano, Adamawa Massif, Cameroon volcanic line, West-central Africa. Geoscience Frontiers, 2020, 11, 665-677.	8.4	6
110	Clarifying source assemblages and metasomatic agents for basaltic rocks in eastern Australia using olivine phenocryst compositions. Lithos, 2021, 390-391, 106122.	1.4	5
111	Reconstruction of primary alkaline magma composition from mineral archives: Decipher mantle metasomatism by carbonated sediment. Chemical Geology, 2021, 577, 120279.	3.3	5
112	Pyroxenite in the mantle source of basanites at the Youkou maar, Adamawa Volcanic Massif (Cameroon Volcanic Line, West Africa). Chemical Geology, 2021, 583, 120478.	3.3	5
113	Dynamic Metasomatism Experiments Investigating the Interaction between Migrating Potassic Melt and Garnet Peridotite. Geosciences (Switzerland), 2021, 11, 432.	2.2	4
114	Evidence for Archean ocean crust with low high field strength element signature from diamondiferous eclogite xenoliths. Developments in Geotectonics, 1999, 24, 317-336.	0.3	2
115	The Role of Blueschist Stored in Shallow Lithosphere in the Generation of Postcollisional Orogenic Magmas. Journal of Geophysical Research: Solid Earth, 2020, 125, e2020JB019910.	3.4	2
116	Transformation from oxidized to reduced alkaline magmas in the northern North China Craton. Lithos, 2021, 390-391, 106104.	1.4	2
117	Ancient continental blocks soldered from below. Nature, 2021, 592, 692-693.	27.8	1

118 Ancient Plate Tectonics. , 2014, , 1-12.